Journal of Cellular Biochemistry 60:246–259 (1996)

Loss and Shedding of Surface Markers From the Leukemic Myeloid Monocytic Line THP-1 Induced to Undergo Apoptosis

S.B. Brown, R.M. Kluck, and K.A.O. Ellem

Queensland Cancer Fund Research Unit (S.B.B., K.A.O.E.) and Liver Unit (R.M.K.), Joint Experimental Oncology Program, Queensland Institute of Medical Research, The Bancroft Centre, P.O. Royal Brisbane Hospital, Brisbane, Australia 4029

Abstract Previous studies have established that a relationship exists between apoptosis and cell surface (ecto-) peptidase activity. Thus dose-dependent increases were found both in ectopeptidase activities and in the proportion of cells undergoing apoptosis in HeLa cell monolayers after exposure to UV and other perturbants causing arrest of DNA synthesis (indirectly or directly as a result of DNA damage). The nature of the correlation made no distinction as to whether an increase in peptidase activity was causal of, or consequential to apoptosis, nor whether the increase was a general response by all cells. As a wider approach to understanding the possible role played by ectopeptidases in apoptosis, we report the effect on expression of a known ectopeptidase, aminopeptidase N (CD13), by a myelomonocytic cell line induced to undergo apoptosis. Using THP-1 cultures exposed to low concentrations of ethanol, we used FACS technology to sort for early apoptotic cells that have an increased ability to sequester the vital dye Hoechst 33342 while excluding nonvital dyes. Apoptosis was verified by light, fluorescence, and transmission electron microscopy, and the presence of DNA fragmentation. These early apoptotic cells showed a significant loss in CD13 labeling. Another surface marker, CD33, behaved similarly, whereas CD14 was lost globally, and not just by the apoptotic cells. Peptidase assays confirmed that an aminopeptidase was shed into the bathing media and that this activity was inhibitable both by bestatin and by a CD13 neutralizing monoclonal antibody. In treated cells, there was no evidence for an increase in cell surface protease activity directed toward a highly aliphatic nonapeptide substrate used as a model for TGF-α scission from its precursor form. However, other cell surface proteases of different specificity are presumably responsible for the observed shedding of CD13.

Key words: apoptosis, CD13, CD14, CD33, aminopeptidase N shedding, ethanol/THP-1 cultures, ectopeptidase activation

A constellation of soluble polypeptide products released by enzymatic hydrolysis from cell surfaces has been collated by Ehlers and Riordan [1991] and provides a rich source of juxtacrine, paracrine/autocrine, and endocrine mechanisms for intercellular communication. Activation of these mechanisms will most likely be regulated by controlling the function of the hydrolytic enzymes involved in releasing the soluble proteins from their membrane forms such as the mature forms of various members of the EGF family, CSF-1, TNF-α, and KL, all excised from transmembrane precursors by proteolytic cleavage [e.g., Massagué and Pandiella, 1993]. In pursuit of the putative transforming growth factor-α-ase ("TGF-α-ase") responsible for the release of TGF-α from HeLa cell surfaces following low dose UVC exposure [e.g., Ellem et al., 1988; Brown et al., 1992, 1993], we found that not only candidate cell surface metalloprotein endopeptidase activity but also ecto-aminopeptidase (not CD13) activity increased severalfold after the UVC exposure. Furthermore, we discovered a strong correlation between the proportionate incidence of apoptosis in the exposed cells and the magnitude of both amino- and endopep-

Received April 3, 1995; accepted June 23, 1995.

Dr. Brown is now at the Division of Renal and Inflammatory Disease, Department of Medicine, University of Nottingham, UK NG72UH.

Abbreviations used: EGF, epidermal growth factor; CSF-1, colony stimulating growth factor-1; TNF-α, tumor necrosis factor-α; KL, kit ligand.

Address reprint requests to Dr. K.A.O. Ellem, Queensland Cancer Fund Research Unit, Joint Experimental Oncology Program, Queensland Institute of Medical Research, The Bancroft Centre, P.O. Royal Brisbane Hospital, Brisbane, Australia 4029.

tidase activity in the intact cultures. This correlation was seen following treatment with either UVC or a variety of inhibitors of macromolecular synthesis such as mitomycin C, actinomycin D and cycloheximide [Brown et al., 1994]. While we are engaged in the process of determining whether the surface protease activation of HeLa cells is global in distribution or is unique to cells following the apoptotic pathway, we sought to examine whether such changes in cell surface function are generally found in cells of different lineage, undergoing apoptosis resulting from different stressors.

The human leukemic myelomonocytic cell line THP-1 has several surface antigens for which standard immuno-probes are available and one of which (CD13) has well-characterized aminopeptidase-N activity. Like many hematopoietic cell types, THP-1 cultures are particularly susceptible to the induction of apoptosis, and one of us has been studying ethanol as an apoptotic agent [Kluck et al., in preparation]. The reported correlations between malignant melanoma cell invasion and the cell surface expression of CD13 [Menrad et al., 1993; Saiki et al., 1993] became interpretable with the observation that anti-CD13 antibodies inhibit invasion and metastasis. Although unlikely to digest the components of extracellular matrix (ECM) or basement membrane by virtue of its N-terminal exo-proteolytic activity, CD13 (which is released and tightly bound to ECM) [e.g., Menrad et al., 1993] may trigger a proteolytic cascade thereby clearing a pathway for the migratory malignant cell. The constitutive presence of CD13 on the surface of a naturally migratory cell like THP-1 may also act to weaken ECM to allow cell passage. It therefore becomes of particular interest to observe what changes might occur at the surface of THP-1 cells undergoing apoptosis. It might be thought that CD13 activity would be irrelevant to the expected stationary status of a cell which had been immobilized by crosslinking of its cytoplasmic proteins. Comparison with two other markers—CD14 and CD33—was thought to be useful in obtaining some idea of the homo- or heterogeneity of the response of several different surface proteins during apoptosis.

Both global and apoptosis specific loss of surface markers occurred. No evidence of endopeptidase activation for the peptide substrate used in previous studies was found. However, since CD13 is readily removed from untreated THP-1 cells by exogenously supplied proteases the observed shedding of aminopeptidase N (CD13) from apoptotic cells into the culture medium, implies the activation of a protease at the THP-1 cell surface as part of the apoptotic program of these cells.

MATERIALS AND METHODS

Materials

Unconjugated mouse anti-human CD13 monoclonal antibody (mAb), clone WM15 was a gift from Dr. K. Bradstock (Westmead Hospital, N.S.W., Australia). FITC-labeled sheep anti-mouse (FSAM) was from Silenus (Hawthorn, Vic, Australia). Mouse antihuman CD14 (clone Mem-18) and CD33 (clone P67.6), both unconjugated, were from Becton-Dickinson (San Jose, CA). Hoechst 33342 was from Calbiochem (San Diego, CA).

Methods

Cell culture. The leukemic myeloid progenitor cell line THP-1, obtained from Dr. Toni Antalis (Q.I.M.R.), was maintained in RPMI-1640 containing antibiotics (Gibco, Grand Island, NY) supplemented with 10% fetal bovine serum (FBS) heat inactivated at 56°C for 30 min. THP-1 cultures were maintained typically at a density greater than 4×10^5 cells/mL and in this way were restricted from activation as assessed by clumping or attachment to the culture flask. THP-1 cultures were routinely assessed to be free of *Mycoplasma* contamination according to the protocol of Chen [1977] following cytospin and fixation of cells to a glass slide.

Morphological identification and quantitation of apoptosis. THP-1 cells were processed for light and electron microscopy by fixation in 3% glutaraldehyde in 0.1 M sodium cacodylate buffer, pH 7.2, for at least 30 min, as previously described [Kluck et al., 1993]. Fixed cells were smeared on coated glass slides, air-dried, and stained with hematoxylin and eosin (H&E) for analysis of apoptosis or necrosis by light microscopy. The percentage of cells that were normal, apoptotic, and necrotic was assessed in random fields and for the most part, a total of 200 cells per sample were counted, with the operator unaware of the sample identity. Apoptosis was identified by markedly condensed chromatin, which was either within a single nucleus or in multiple nuclear fragments, characteristic of apoptosis [Kerr et al., 1972; Walker et al., 1988]. Cells in late apoptosis exhibiting eosinophilic cytoplasm were included in the apoptosis counts. Necrotic cells exhibited dispersed

chromatin in association with eosinophilic cytoplasm. Fixed cells were further processed for transmission electron microscopy (TEM) as previously described [Harmon et al., 1990].

DNA electrophoresis. Analysis of DNA cleavage to oligonucleosomal fragments was performed as previously described [Kluck et al., 1993], whereby DNA was extracted and underwent electrophoresis in 1.7% agarose for 1 h at 60 V (running buffer 40 mM Tris–acetate, 1 mM EDTA, pH 8.0). Cleavage to high-molecular-weight fragments was assessed using modifications of methods described by Walker et al. [1994]. Treated cells (1×10^6) were pelleted to a 25-μl volume, and 25 μl of 2% sodium dodecyl sulfate (SDS) in ddH_2O was added. Using a pipette tip amputated to minimize DNA shear, the sample was gently mixed and placed in the wells of agarose gels, and the wells sealed with 1% low melting point agarose. Either conventional electrophoresis at 40 V for 22 h in 0.8% agarose (running buffer 40 mM Tris–acetate, 2 mM EDTA, pH 8.5), or pulsed field electrophoresis for 22 h in 1% agarose at 200 V (running buffer 20 mM Tris–borate, 1 mM EDTA, pH 8.5, prechilled to 4°C), with the ramping rate changing from $T_1 = 0.5$ s to $T_2 = 50$ s employing the BioRad CHEF-DR II system, was performed.

FACS analysis and sorting. Induction of apoptosis was attained by the addition of ethanol. THP-1 cells were first removed from a stock culture and collected by centrifugation at 200*g* before resuspending by trituration to a density of 1×10^6 cells/ml in fresh media prewarmed to 37°C and containing ethanol to the desired percentage by volume. Only stock cultures in which the vast majority of suspended cells were monodisperse were used. Cells were typically aliquoted into 20-ml capped sterile tubes, sealed with parafilm, and incubated in a 37°C warm room (the ratio of volume of media to air was typically no less than 5:1). In the event that cells were subsequently sorted or analyzed by FACS, the parafilm seal was broken 10 min before time, and Hoechst 33342 (50 μg/ml stock in PBS) added to the culture to a final concentration of 0.5 μg/ml.

In order to separate THP-1 cell populations into subpopulations representing normal, early apoptotic and late apoptotic cells, the difference in intracellular concentration of Hoechst 33342 (and thus viable DNA staining), which occurs in cells engaged in apoptosis compared with normal cells was used [Darzynkewicz et al., 1992; Sun et al., 1993; Cohen et al., 1993; Ormerod et al., 1993], together with propidium iodide staining of nonviable cells to separate the late apoptotic cells from those still in an early apoptotic state.

Prior to sorting, THP-1 cells, treated with ethanol or not, and incubated with Hoechst 33342, were centrifuged (200*g*, 4°C) and washed once with ice-cold phosphate-buffered saline (PBS). Cells were then resuspended in ice-cold PBS containing either bovine serum albumin (BSA) at 4 mg/ml (PBS/BSA) and primary antibody where appropriate (see below), or propidium iodide at 0.1 μg/ml. In all cases, cells were resuspended at approximately 5×10^6 cells/ml.

Cells were analyzed and sorted by a FACS-Vantage (Becton-Dickinson) employing LYSIS-II software. The instrument was configured with the primary Krypton laser emitting at 352 nm for Hoechst measurements and with a secondary argon-ion laser emitting at 488 nm by which forward and side light scatter was determined, and emitted red (630 nm, PI) and green (520 nm, FITC) fluorescence was recorded. Samples were analyzed at 4°C, the entire fluid system having been precooled and maintained via a refrigerated circulating water bath. Cells were analyzed and sorted using a discrimination of one drop either side of a counted cell.

Sorted cells (typically 1×10^6) were collected into 5-ml tubes containing 1 ml of 100% FBS (heat inactivated for 1 h at 70°C) and maintained at 4°C. Following collection, cells were centrifuged, washed twice with PBS/BSA, and suspended in 200 μl of the same solution from which aliquots were then removed and to which primary mAbs were added for incubation. In all labeling experiments, cells were first incubated for 30–120 min at 4°C with the primary mAb, invariably 10 μl per 1×10^6 cells. Cells were then washed twice with ice-cold PBS/BSA before the addition of a secondary, polyclonal FSAM antibody. After 30 min incubation, cells were washed twice with ice-cold PBS before final suspension in ice-cold PBS containing PI, for immediate FACS analysis.

Peptidase assay and quantitation of peptide hydrolysis. Peptidase assays were performed as previously described [Brown et al., 1992, 1993]. Briefly, a nonapeptide synthesized to be cognate with the N-terminal cleavage site of mature TGF-α and containing an added N-terminal tyrosine to permit radio-iodination (H-YVAAAVVSH-NH2, denoted P9 herein), was

incubated (30 min, 37°C) with 100–200 μl of THP-1 cells washed free of conditioned media and ethanol, and then suspended in HBSS at a density of 1×10^6 cells/ml. After the appropriate incubation time, a 45-μl aliquot of the assay solution (supernatant) was removed and immediately spotted onto a multichanneled TLC plate (Whatman, LK6D). Titrations of the inhibition of CD13 aminopeptidase activity with bestatin and mAb's were performed by pre-incubating the inhibitors with the cells at the desired concentration for 5 min prior to the addition of the P9 substrate.

To determine the level of peptidase activity secreted or shed by THP-1 cells treated with ethanol or not, cells were removed from their media, resuspended and washed once in HBSS, before final resuspension in HBSS at 2.5×10^6 cells/ml. Aliquots (200 μl) were either removed immediately and assayed in the presence of P9 and inhibitors as above, or left as a suspension for 30 min at 37°C for shedding to occur. Cells were then removed by centrifugation and the resulting supernatant assayed with P9 and inhibitors for 30 min.

Fully loaded TLC plates were developed with butanol–acetic acid–water (100:10:30) (BAW) to allow for the separation of P9 from its products. The Rfs of all iodinated peptides from Y, YV, YVA, . . . , etc. (denoted P1, P2, P3, . . .) were determined, to allow the site of the scissile bonds to be assessed [Brown et al., 1992]. Visualization of the TLC plate was performed by exposure to a storage phosphorscreen (Kodak) and was realized by phosphorimaging (Molecular Dynamics, Sunnyvale, CA). Quantitation and analysis of results were performed with ImageQuant software (Molecular Dynamics, Version 3.15).

RESULTS

Apoptosis of THP-1 Cells Following Incubation With Ethanol

Apoptosis develops in THP-1 cells following the addition of ethanol at 2–6% (v/v) to the culture media for 4 h (Fig. 1), with few cells exhibiting necrosis. Higher ethanol concentrations induce necrosis. This concentration effect of ethanol on the type of cell death is seen with several cell types [Kluck et al., in preparation].

Verification of the Presence of Apoptosis

As it is important to establish firmly the identification of apoptosis, this was done by several methods. UV light microscopy of cells stained with Hoechst 33342 for sorting by flow cytometry-revealed tell-tale patterns of nuclear chromatin condensation and margination. This morphology was also routinely seen in these cells after fixation and staining with H&E.

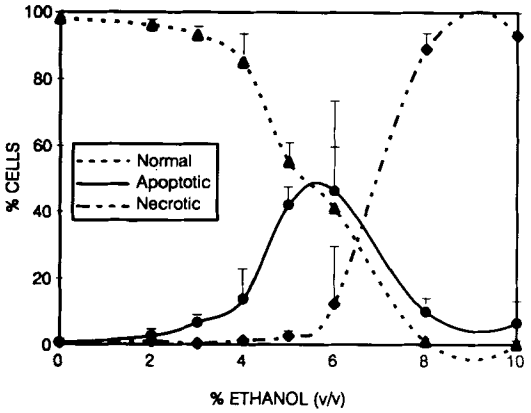

Fig. 1. Effect of increasing ethanol concentration (v/v) on the level of apoptosis present in THP-1 cultures following a 4-h incubation at 37°C. Morphological assessment of cells as being normal (.....), apoptotic (___), and necrotic (-··-) was as described in Methods. Percent cells were determined from random fields and a minimum of 200 H&E-stained cells counted. Mean and SD of three experiments.

Of critical importance, TEM of apoptotic THP-1 cells displayed the features characteristic of apoptosis (Fig. 2B) [Kerr et al., 1972; Walker et al., 1988]. Both the nucleus and the cytoplasm were condensed, and both exhibited budding. Organelles were intact, clear vacuoles were present, and cell surface microvilli were decreased. Nucleolar disintegration to two components, clusters of dispersed granules and compact granular masses, was evident. The most characteristic feature, however, was the redistribution of the heterochromatin to form condensed masses which lay adjacent to the nuclear membrane, leaving a uniformly clear but still spotty centre of the nucleus. The chromatin is not as strongly condensed nor as sharply marginated as in other cell types undergoing apoptosis; this has also been noted in apoptotic mouse embryonic cells following serum depletion [Tomei et al., 1993], and in apoptotic HeLa cells following treatment with actinomycin D [Kerr et al., 1995].

Instead of internucleosomal DNA cleavage producing the ladder patterns frequently associated with apoptosis, DNA degradation after 4-h exposure to $<6\%$ ethanol produced large-molecular-weight fragments of broad range, centered at 30–50 kb pairs and were not seen in untreated cultures (Fig. 3A,B). This pattern of DNA degradation has been shown to precede the inter-

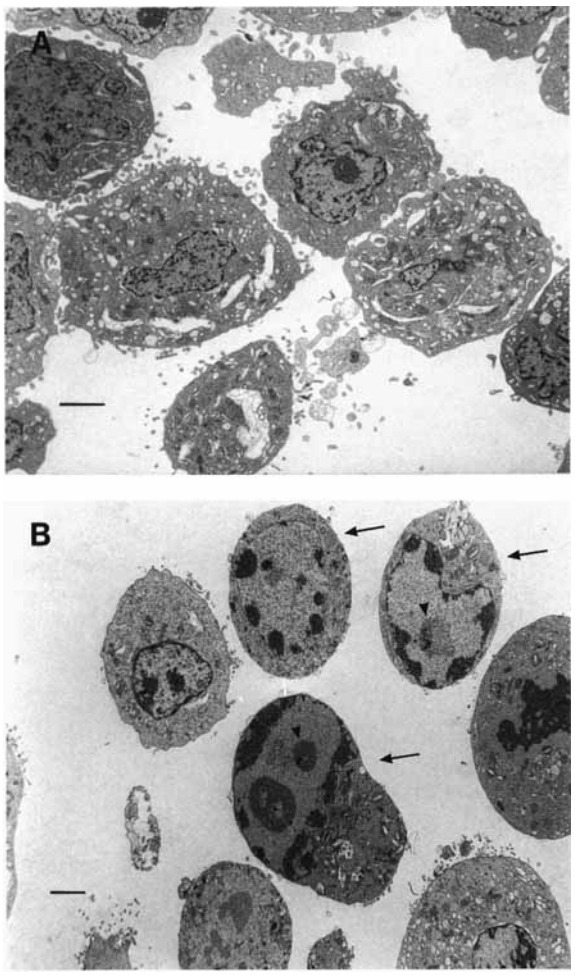

Fig. 2. Transmission electron microscopy of apoptosis in THP-1 cells treated with 3% ethanol for 4 h. **A:** Normal cells sorted as R1 population. ×3,000. **B:** Apoptotic cells enriched in R2 sorted population exhibit distinct morphological features of apoptosis. ×2,500. Apoptotic cells (*arrow*), nucleolar remnants (*arrowhead*). Bar = 2 μm.

nucleosomal cleavage seen in most apoptotic systems [Oberhammer et al., 1993; Cohen et al., 1994] and is present in apoptotic cells, even in the absence of internucleosomal cleavage (Oberhammer et al., 1994). A similar pattern of high-molecular-weight DNA fragmentation can be associated with necrosis in some cell systems (e.g., with 8% ethanol 4 h, Fig. 3B, lane 5), but not in others [Kluck, unpublished], suggesting that some biochemical features of apoptosis and necrosis may be related.

Sorting of Apoptotic Cells

To sort for apoptotic cells, THP-1 cells were first assessed by FACS for differential uptake of Hoechst 33342 and the exclusion or not of propidium iodide. FACS of cells treated for 4 h with 3% ethanol (Fig. 4) revealed three distinct populations in a two-dimensional cytogram for Hoechst content versus propidium iodide, uptake. The R3 population is characterized by an inability to exclude propidium iodide and was indicative of cells that had lost plasma membrane integrity. The R1 population was identifiable with normal cells by coincidence of its position with that of untreated paired controls. R2 represented a novel and distinct population arising as a consequence of ethanol treatment. Although Figure 1 suggests that treatment with 4% ethanol for 4 h was optimal for inducing apoptosis, we found consistently that such treatment resulted in too large an R3 population, typically >60% of all gated cells. This was considerably reduced if the cells were treated alternatively with 3% ethanol for 4 h, which generally left the proportion of cells to be found in R2 unaltered. All attempts to increase the separation of the R1 and R2 populations were ineffective when variables such as temperature, time of incubation and the concentration of Hoechst 33342, were manipulated.

R2 Is a Transitional Early Apoptotic Pool

Morphological assessment of the three sorted populations by fluorescence microscopy indicated that the R1 population did indeed comprise normal cells indistinguishable from untreated cells. The R3 population was wholly apoptotic as discerned by Hoechst staining of highly pyknotic and marginated nuclei and was further characterized as late apoptosis by the complete inability of these cells to exclude nonvital dyes, as verified by the addition of trypan blue. The R2 population also revealed an apoptotic population but, unlike R3, most of these sorted cells excluded trypan blue (81% ± 9%). The finding that up to 20% of the cells in the R2 population subsequently stained with trypan blue (but had excluded propidium iodide prior to sorting) was attributed to the physical stress of collection and to the time taken to collect a sizeable number of cells, typically 3–5 h for 1×10^6 cells. Morphological assessment of apoptosis in the sorted cells was made following fixation and staining with H&E (Table I) and confirmed that the R1 sorted population contained predominantly normal cells and that the R2 sorted population of cells was predominantly apoptotic. Further confirmation that the FACS-sorted region R1 represented "normal" cells and R2 an "early" apoptotic pool was provided by electron microscopy of the sorted cells (Fig. 2A,B).

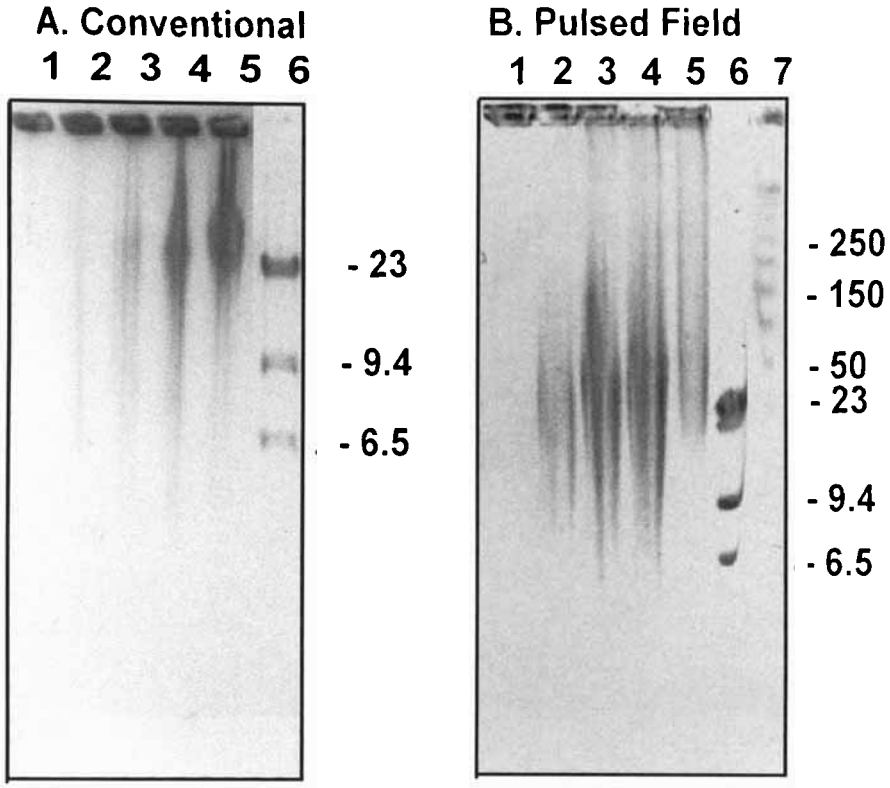

Fig. 3. High-molecular-weight DNA fragments confirm apoptosis in ethanol-treated THP-1 cells. Cells were analyzed after 4-h incubation with a range of ethanol concentrations followed by lysis in 1% SDS and either (**A**) conventional gel electrophoresis at 40 V for 22 h or (**B**) CHEF pulsed field gel electrophoresis as described in Methods. Conventional gel samples are treated with 0, 2, 4, 5, 6% ethanol (*lanes 1–5*), λ-*Hind*III digest (*lane 6*). Pulsed gel samples are treated with 0, 4, 5, 6, 8% ethanol (*lanes 1–5*), λ-*Hind*III digest (*lane 6*), concatamerized λ ladder (*lane 7*). Molecular weights are in kbp units. Images are computer-generated negative prints of ethidium bromide-stained gels, the negatives being used because of better contrast than in the positive prints.

Having established that R2 represented an early apoptotic population, an attempt was made to see whether by varying the length of time the cells were incubated with ethanol, a larger R2 population could be obtained, thereby reducing the time necessary to sort cells without a concomitant loss in purity. The data of Figure 5, taken from FACS analyses, indicated that the most favourable time to sort for early apoptotic cells was at ~3 h following the addition of ethanol. Beyond 4 h, a constant level of apoptosis is apparent for up to 8 h and is presumably maintained by a flux of cells from an ever diminishing R1 pool, to an increasing R3 subpopulation.

Loss of CD13 on Sorted Apoptotic THP-1 Cells

Ethanol-treated cells (3%, 3 h) sorted and collected by FACS at 4°C were incubated at 4°C either with an unconjugated mouse mAb raised against human CD13 (clone WM15) or with its IgG-1 isotyped control, and both were followed by an FITC-conjugated sheep anti-mouse Ab (Fig. 6). Outstanding was the 69% reduction in anti-CD13 fluorescence ($P = 0.0001$) of the mode of the early apoptotic (R2) population. Nonviable (R3) cells had an even greater modal decrease (92%) of the immunofluorescence signal from the normal (R1) population. Attempts to duplicate this result with an alternative mAb against human CD13 (clone 3D8) were inconclusive, as an IgG-2a isotyped control for 3D8 was shown to bind nonspecifically and differentially between the various sorted populations, increasing from R1 to R3 (data not presented).

Anti-CD13 (WM15) Inhibits Most Cellular Ecto-aminopeptidase Activity

Before investigating the possibility that CD13 was "shed" into the media we first assessed the ability of WM15 to inhibit aminopeptidase activity of untreated intact control THP-1 cells. Figure 7A,B depicts thin-layer chromatograms (TLC) of a series of assays of the surface pepti-

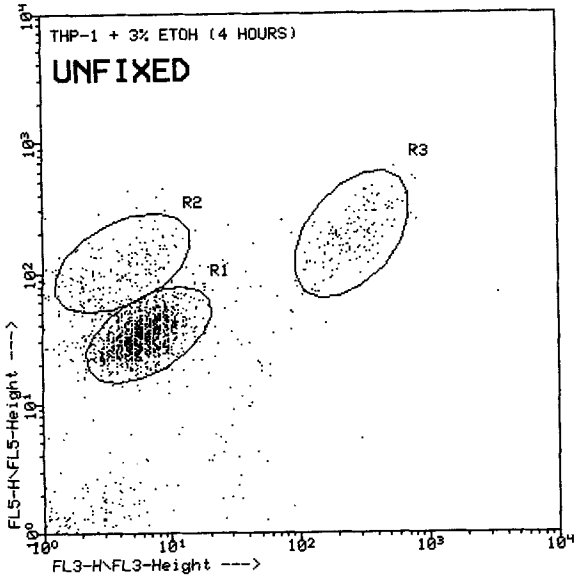

Fig. 4. Bivariate histogram showing the separation of three distinct cell populations sorted by flow cytometry. Unfixed cells were sorted according to their Hoechst 33342 uptake (y-axis) versus propidium iodide (x-axis) as described in Methods. Cells were gated on forward and side light scatter so as to exclude debris and subcellular particles.

TABLE I. Morphological Assessment[a] of FACS-Sorted THP-1 Cell Populations

	% Normal	% Apoptosis	% Necrosis
Exp 1			
EtOH total unsorted	79	17	4
Control R1 sort	98	1	0
EtOH R1 sort[b]	—	—	—
EtOH R2 sort	20	78	3
EtOH R3 sort	0	98	5
Exp 2			
EtOH R1 sort	95	5	0
EtOH R2 sort	8	91	1

[a]Sorted cells were fixed and stained with H&E and 200 cells counted for quantitation.
[b]No cells remained after H&E processing.

dase activity of intact cells in the presence of increasing concentrations of anti-CD13 or bestatin. Quantitation for percent substrate hydrolysis (Fig. 7C,D, respectively) was determined exclusively from the formation of P1 as product and does not take into account the formation of other products. Interestingly, WM15 specifically inhibited the production of P1, and not P2 or P3, whereas bestatin affected the accumulation of P2 and P3, as well as the anticipated product, P1, at the highest concentration used.

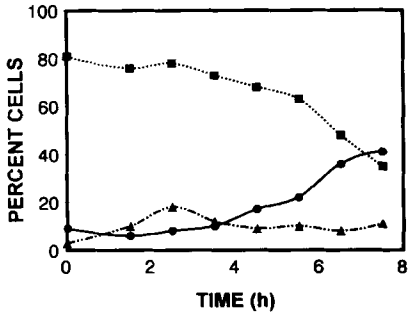

Fig. 5. Time course for ethanol induction of apoptosis as determined from FACS analyses. Gates were set for viable, R1 (■---■), early apoptotic R2 (▲···▲), and nonviable apoptotic, R3 (●---●) cell populations at the indicated times following addition of ethanol at 3% to cultures.

The titration curve of Figure 7C indicates that 2 μl of WM15 per 5 × 10^5 cells was sufficient to inhibit the available ecto-aminopeptidase activity by 60% at the cell surface, but that further additions of mAb had little effect. As a comparison, bestatin, known to be a potent inhibitor of aminopeptidase [Suda et al., 1976], was shown to inhibit aminopeptidase activity to a similar degree (77%) at a concentration of 40 μg/ml (Fig. 7D). The specificity of WM15 confirms that aminopeptidase N (CD13) was the dominant THP-1 surface aminopeptidase activity. Titration of THP-1 with an IgG-1 isotyped control mAb had no effect on the level of assayable peptidase activity (data not shown).

Ethanol-Treated THP-1 Cells Shed CD13 into Media

The peptidase assays (Fig. 8A) showed decreased cell surface-associated aminopeptidase activity ($P = 0.024$) and a significant ($P < 0.005$) increase in the release of aminopeptidase activity (more than twofold in 30-min exposure) into the bathing media of ethanol-treated cells, most obvious after normalization (Fig. 8B). Quantitation of P1 product formation revealed that, in control samples, as much as 25% (white component of each histogram bar) of the total activity (total height of each bar) arose from soluble activities and was not cell associated. The shaded component of each bar represents the fraction of activity remaining after subtracting out that component which was directly attributable to enzyme released into the HBSS supernatant during the course of an intact cell assay. The values subtracted are, however, a significant overestimation of the time average release of activity, as the soluble peptidase component was

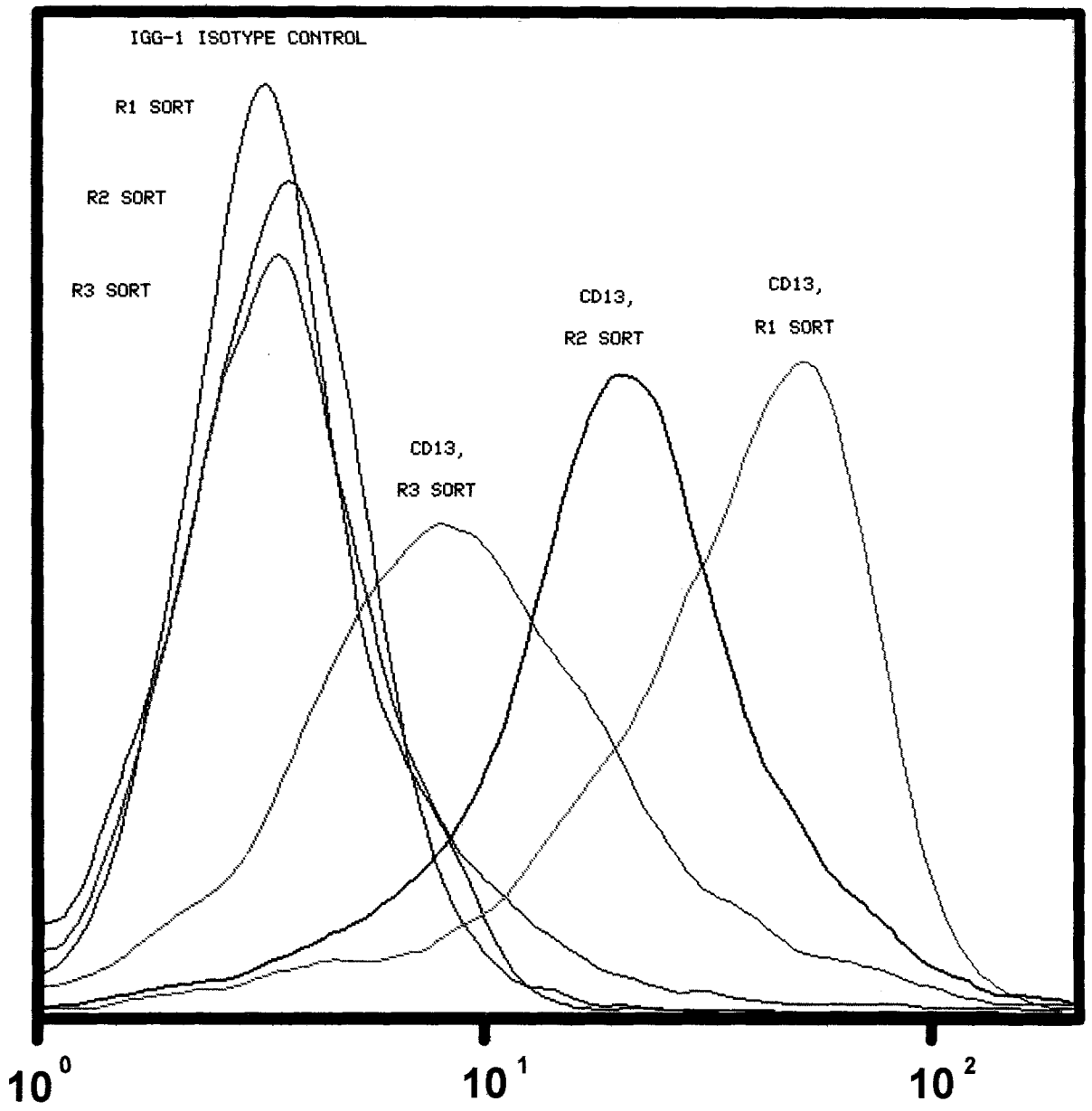

Fig. 6. Cell surface expression of CD13 as assessed by FACS analysis. Sorted cell populations were labelled with an unconjugated mouse anti-CD13 mAb, clone WM15, and conjugated with an FITC-labeled sheep antimouse Ab with all steps performed at 4°C. Sorted cells were also labelled with a mouse unconjugated IgG-1 isotype mAb followed by FSAM for control reference. The abscissa is in log fluorescence intensity units. The ordinate is in arbitrary units for each curve, representing cell numbers in the distribution.

assessed with a 30-min assay after 30-min exposure of the cells to HBSS. The resulting non-white component of each histogram bar is therefore interpreted as representing the activity associated with the cell. The significant ($P < 0.02$) loss of total activity (18.9% loss) found with ethanol treatment (Fig. 8A) is attributed to ethanol itself being inhibitory for metallopeptidases (unpublished results). Both released and total aminopeptidase activity were inhibited 50–60% by bestatin (all values $P < 0.001$), and specific aminopeptidase N anti-

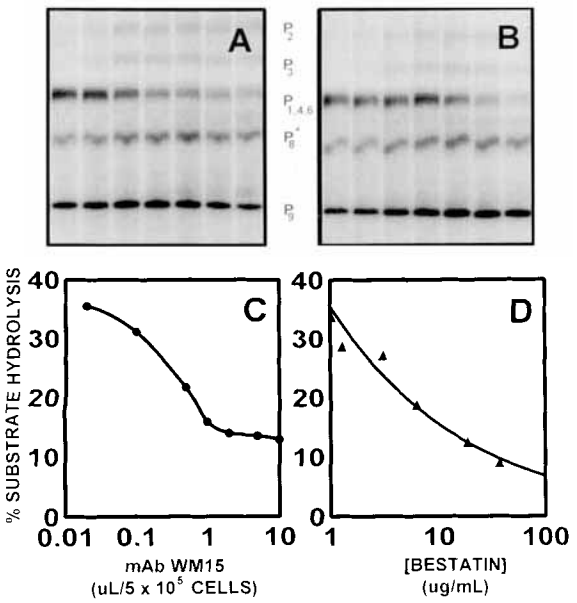

Fig. 7. Titration of cell surface aminopeptidase activity with antibody (**A**) and bestatin (**B**). The lanes from left to right correspond to the data points (from L to R) in **C** and **D**, respectively. THP-1 cells in HBSS were assayed for aminopeptidase activity by the generation of free iodinated tyrosine (P1) in the presence of increasing concentrations of the anti-CD13 mAb WM15 (**A**) and the aminopeptidase inhibitor bestatin (**B**) as revealed by TLC. The substrate P9 and the contaminant P8* are seen to be converted predominantly to P1 and to a lesser extent P2 and P3 (see Methods). Quantitation of activity was determined from duplicates of separate assays (four determinations, two each of the same TLC) for each of the two inhibitors respectively (Panel C and D). Note that the x-axes for both **C** and **D** are logarithmic and range from 0.02 to 10 μl and 1 to 38 μg/ml for both, respectively.

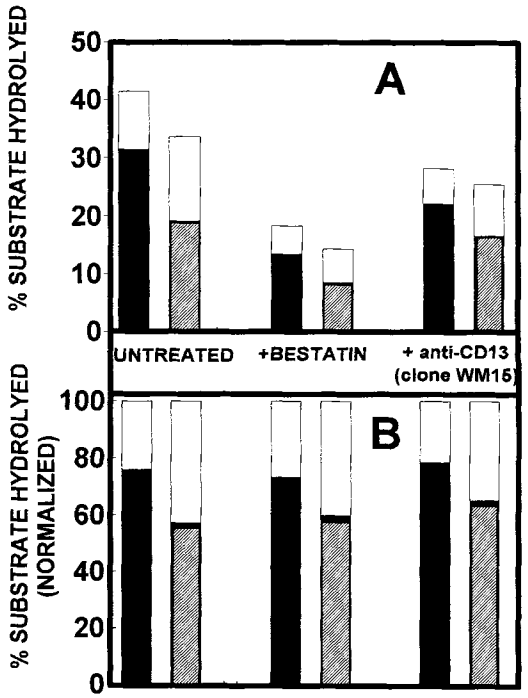

Fig. 8. Release of peptidase activity to the supernatant of THP-1 cells after ethanol treatment. The white rectangle at the top of each histogram bar represents the aminopeptidase activity shed by the indicated experimental group of cells (all at 2.5×10^6 cells/ml) during 30-min incubation in HBSS at 37°C, prior to peptidase assay of the supernatant. The solid black bars indicate the cell surface aminopeptidase activity of control cells and the shaded bars that of an equal number of cells exposed to ethanol (3% for 3 hr) prior to assay for total or shed enzyme. **A:** Data for the percentage hydrolysis of P_9 to P_1 (aminopeptidase activity) in the absence (untreated) or presence of bestatin (10 μg/ml) or WM15 (2 μl). **B:** Data from **A** have been normalized to a total activity of 100% for each group to compare the ratios of shed to cell-associated aminopeptidase activity in each experimental group (thus eliminating the confusing effect of ethanol inhibition of aminopeptidase). Rather than increase the complexity of the figure with multiple error bars, the significance of relevant differences (by *t*-test) between the results embodied in the histograms is quoted in the text where this figure is discussed.

body (WM15) inhibited this activity in both groups from 24% to 40% ($P = 0.01$–$P < 0.001$).

Some THP-1 Cell Surface Markers Behaved Differently

For comparison with the CD13 data, we have explored the fate of two other THP-1 surface markers. Control and ethanol-treated cultures, following incubation with Hoechst 33342, were washed free of media with ice-cold PBS/BSA and incubated at 4°C on ice for 60 min with mAbs raised against human CD13, CD14 or CD33 and then with FITC-labeled antimouse IgG. FACS analysis of the various labelled cells are presented in Figure 9. Where the data are strictly gated on a combined R1 and R2 pool, this is designated R4 for easier comparison with the IgG1 mAb control of untreated cells and the treated cells incubated with specific mAbs (anti CD13-WM15, anti-CD14-MEM-18 and anti-CD33-Leu-M9).

Anti-CD13 results (Fig. 9, CD13, left), consistent with the data of Figure 6, showed that a majority of the ethanol treated population expressed CD13 at the same level as untreated cultures,[1] but that a subpopulation had a much lower anti-CD13 labeling, forming a shoulder on the left side of the ethanol treated cell distribu-

[1]Examination of Figure 9, CD13 *right panel* reveals that those cells treated with ethanol and gated on R1 alone exhibit a small shoulder to the left and that those gated on R2 have a bimodal distribution, one peak with fluorescence intensity approximately 30% of the control mode, while the other was coincident with untreated cells. This suggests a degree of overlap between the two population.

tion curve. This CD13-deficient population stained brightly with H33342 and was thus made up of early apoptotic cells (R2). CD13 is thus preferentially lost from early and late apoptotic cells. Anti-CD33 data (Fig. 9, CD33) yielded curves similar to those of CD13 indicating that this surface marker is also lost only during the process of apoptosis but, unlike CD13, Hoechst staining fully discriminated between high and low CD33-staining populations (Fig. 9, CD33, right).

The data from anti-CD14 studies (Fig. 9, CD14, left), however, were different. The ethanol-treated cell population was unimodal and showed on R1, R2, and R3 analysis that the population of cells lost stainable CD14 from their surfaces equally (Fig. 9, CD14, right) and thus represented a global effect of ethanol on THP-1 cultures and was not an effect unique to the apoptotic subpopulation.

DISCUSSION

In order to investigate changes in cell surface peptidase activity during apoptosis, we employed the THP-1 myelomonocytic cell line, which is known to express an ecto-aminopeptidase for which a specific mAb is available. This was prompted by our previous finding that cell surface peptidase activities of HeLa cultures increases following a variety of insults which cause inhibition of macromolecular synthesis and which was accompanied by dose-dependent occurrence of apoptosis [Brown et al., 1994]. Those studies revealed that a significant contributor to the observed increase in peptidase activity was that with aminopeptidase specificity. The degree of increase in ecto-aminopeptidase activity correlated with the proportion of cells in the culture found to be apoptotic but that remained impermeable to nonvital dyes. Studies had also suggested that the aminopeptidase activity of interest was most likely that of a metallopeptidase for which aminopeptidase-N (CD13) was a potential candidate. Monoclonal antibodies to this particular surface marker indicated the absence of any significant immunolabeling of HeLa cultures for CD13, so we pursued CD13 expression in the leukaemic myelomonocyte cell line THP-1, known to be strongly positive for it.

The present studies have shown that apoptosis was readily induced in THP-1 cultures by treatment with ethanol at 2–6% (v/v), as has been previously observed in HL60 cells treated with 6% (v/v) ethanol [Lennon et al., 1991] and generally at lower concentrations in other hematopoietic cell lines [Kluck et al., in preparation]. By employing flow cytometry [Sun et al., 1992; Cohen et al., 1993; Ormerod et al., 1993], we were able to resolve three populations of cells based on the differential retention of the DNA binding dye Hoechst 33342 and the ability to exclude the nonvital dye propidium iodide. The R1 population of low Hoechst 33342 and PI staining represented normal cells, while the R2 population with high Hoechst and low PI staining were in early apoptosis and the R3 population with high staining with both dyes were late, nonviable apoptotic cells. These assignments were confirmed by morphological examination of the sorted cell populations. The sorting of normal cells (R1) from that of early (R2) or late (R3) apoptosis thus enabled the direct analysis of specific surface markers associated with each pool.

Contrary to our initial expectations (based on our experience with HeLa cells) of an increase in the level of CD13 expression by apoptotic THP-1 cells compared with the normal, a significant loss in the expression of surface resident CD13 was observed. This suggests that the expression of aminopeptidase N by THP-1 cells undergoing apoptosis in response to ethanol treatment is depleted and not elevated. Our results further suggest that the mode of CD13 loss was via shedding from the cell surface possibly by the activation of other proteases resident at the cell surface or other enzymes capable of releasing cell membrane anchored proteins [e.g., Ehlers and Riordan, 1991]. CD13 is cleaved at a site near the outer membrane surface by exogenous papain, for example, with no loss of enzyme activity [Louvard et al., 1975]. Recently, Dransfield et al. [1994] showed that apoptotic neutrophils lose the surface expression of CD16, which can be reproduced by exogenous serine protease (elastase) activity, even though the shedding of CD16 as a consequence of neutrophil and natural killer (NK) cell activation is thought to occur as a result of metalloprotease activity [Bažil and Strominger, 1994; Harrison et al., 1991]. Our own studies have intimated that the shedding of TGFα from cell lines of epithelial origin in response to genotoxic challenge correlates with increases in cell surface endopeptidase activity [Brown et al., 1993] and with dose-dependent incidence of apoptosis [Brown et al., 1994]. Like CD16 [Dransfield et al., 1994], the release of

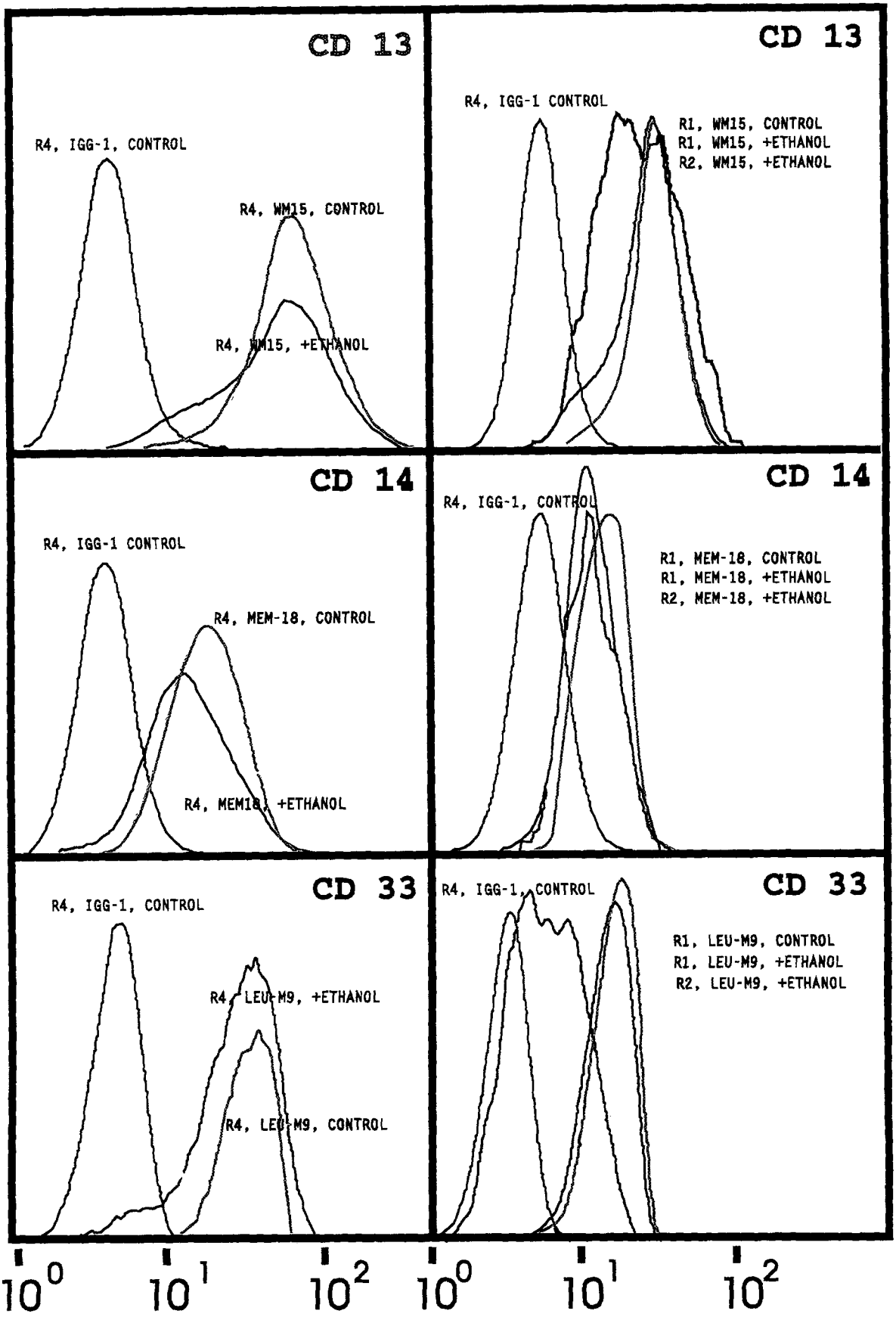
CD 13
R4, IGG-1, CONTROL
R4, WM15, CONTROL
R4, WM15, +ETHANOL
CD 13
R4, IGG-1 CONTROL
R1, WM15, CONTROL
R1, WM15, +ETHANOL
R2, WM15, +ETHANOL
CD 14
R4, IGG-1 CONTROL
R4, MEM-18, CONTROL
R4, MEM18, +ETHANOL
CD 14
R4, IGG-1, CONTROL
R1, MEM-18, CONTROL
R1, MEM-18, +ETHANOL
R2, MEM-18, +ETHANOL
CD 33
R4, IGG-1, CONTROL
R4, LEU-M9, +ETHANOL
R4, LEU-M9, CONTROL
CD 33
R4, IGG-1, CONTROL
R1, LEU-M9, CONTROL
R1, LEU-M9, +ETHANOL
R2, LEU-M9, +ETHANOL
10^0
10^1
10^2
10^0
10^1
10^2

Figure 9.

TGF-α from the cell surface can be effected by exogenous elastase (serine protease) activity [Ignotz et al., 1986; Mueller et al., 1990; Pandiella et al., 1992; Capelluti et al., 1993; Harano and Mizuno, 1994], but we have preliminary evidence that the UV-inducible "TGF-αase" is a metalloprotease. Choudry and Kenny [1991] have also detected an ecto-metalloprotease, from the rat, capable of cleaving TGF-α from its precursor.

It has been suggested that cell death by apoptosis has evolved as a minimally perturbing exitus for unwanted cells, to avoid an unnecessary inflammatory response [e.g., Wyllie, 1993]. Explosion of an apoptotic cell into membrane wrapped apoptotic bodies is swiftly followed by phagocytosis of these bodies by adjacent macrophages or other viable cells. The nature of the change in the membrane surrounding the apoptotic bodies which provokes their rapid uptake by adjacent cells is at present unclear but is of intense interest [e.g., Savill et al., 1993; Rotello et al., 1994]. Duvall et al. [1985] showed that binding of apoptotic thymocytes to isologous peritoneal macrophages appears to be mediated by lectin-like molecules on the surface of the apoptotic cells. Fadok et al. [1992a] found that phosphatidylserine was exposed at the surface of apoptotic lymphocytes and appeared necessary for their ingestion by macrophages via receptors that differ according to the origin of the phagocytic cell [Fadok et al., 1992b]. Differential changes in apoptotic cell membranes, dependent on the cell lineage, microenvironment, and events triggering apoptosis, are likely but are currently unknown. The present work shows that THP-1 cells, of myeloid lineage, lose at least three surface antigens when exposed to the apoptotic stimulus of ethanol at 3% for 3–4 h. Only one of the surface proteins—CD14—was lost globally from all cells in the exposed cultures. The other two surface markers—CD13 and CD33—were lost only by the subpopulation of cells engaged in apoptosis. The loss of cell-associated aminopeptidase activity of CD13 was shown to be due to surface shedding into the culture medium.

By contrast, an ecto-aminopeptidase (not CD13) on HeLa cells increased immediately to rise to a maximum, at 16 h, some two- to fivefold greater than the constitutive level of activity. This was followed, after a 6-h lag, by a similar increase in endopeptidase activities of an elastase type, which maximized 22–24 h after the UVC [Brown et al., 1993]. Since following UVC treatment, there was a strong correlation between the proportion of cells induced to undergo apoptosis and the magnitude of increase in ecto-proteolytic activity, the relationship between the two phenomena needs clarification—whether causal or casual. We are in the process of determining whether these ecto-peptidase activity increases in HeLa cells are global or unique to apoptotic cells. We are also exploring the mechanisms whereby these increases occur, presently known to be of a post-translational nature [Chenevix-Trench et al., 1992]. The purposes of the HeLa ecto-endopeptidase increases following UVC may be the release of membrane bound growth factors (e.g., TGF-α) as originally proposed [Ellem et al., 1988]. The increase in ecto-aminopeptidase activity may relate to cell gearing for repair/division activity, such as increase of amino acid availability by increasing the products of N-terminal peptide digestion [Kenny et al., 1989] and also possibly by enhancing amino-acid transport [Plakidou-Dymock et al., 1993]. It is equally possible that the increase in ectopeptidase activity results from the redistribution of an intracellular pool, and is a component of the apoptotic pathway that allows for the shedding of surface proteins, of which TGF-α is an example.

While it has been difficult to rationalize the role of aminopeptidase N in hematopoietic cells, the recent observation that this enzyme, when shed from malignant cells is tightly bound to extracellular matrix and results in its dissolution [Menrad et al., 1993; Saiki et al., 1993] is perhaps relevant. Thus it is possible that, in the in vivo situation, myelomonocytic cells, rigidified and immobilised by the cross-linking of cytoplasmic proteins as they undergo apoptosis, release their surface aminopeptidase N (CD13) with the resultant digestion of a pocket in the extracellular matrix in which it is embedded,

Fig. 9. Effect of ethanol treatment on the expression of other surface markers. THP-1 cells treated with or without 3% ethanol for 4 h were immunolabeled at 4°C for the indicated CD antigens following incubation in Hoechst 33342 for 10 min at 37°C. The distribution of cells according to the magnitude of the indicated antibody fluorescence (abscissa) is shown for the total viable cell population ($R_1 + R_2 = R_4$) (left column) or for the normal (R_1) and early apoptotic (R_2) subpopulations separately (right column). All panels contain R_4 control stain using the nonspecific monoclonal antibody isotype IgG-1 to gauge the specific immunofluorescence.

thereby increasing the immediate access of surrounding viable cells to ingest the apoptotic "shrapnel."

ACKNOWLEDGMENTS

The invaluable assistance of Ms. Grace Chojnowski (QIMR) is gratefully acknowledged for operating the FACS, as is the expert help of Clay Winterford (Department of Pathology, University of Queensland) with electron microscopy. We would also like to thank Dr Gerald Cohen (MRC Toxicology Unit, University of Leicester) for the suggestion to look for high M.W. DNA cleavage products in the apoptotic system. This work was supported by a grant from the National Health and Medical Research Council of Australia.

REFERENCES

Bažil V, Strominger JL (1994): Metalloprotease and serine protease are involved in cleavage of CD43, CD44, and CD16 from stimulated human granulocytes. J Immunol 152:1314–1333.

Brown SB, Krause D, Townsend E, Ellem KAO (1992): Development of a sensitive peptidase assay: in search of cell associated proteases responsible for the cleavage of preproTGFα. J Cell Biochem 48:411–423.

Brown SB, Krause D, Ellem KAO (1993): Low fluences of ultraviolet irradiation stimulate HeLa cell surface aminopeptidase and candidate "TGFαase" activity. J Cell Biochem 51:102–115.

Brown SB, Kluck RM, Ellem KAO (1994): Induction of cell surface peptidase activity: A global response to cell stress correlated with apoptosis. J Cell Biochem 54:320–331.

Cappelluti E, Strom SC, Harris RB (1993): Potential role of two novel elastase-like enzymes in processing pro-transforming growth factor-α. Biochemistry 32:551–560.

Chen TR (1977): In situ detection of *Mycoplasma* contamination in cell cultures by fluorescent Hoechst 33258 stain. Exp Cell Res 104:255–262.

Chenevix-trench G, Cullinan M, Ellem KAO (1992): UV induction of transforming growth factor alpha in melanoma cell lines is a posttranslational event. J Cell Physiol 152:328–336.

Choudry Y, Kenny AJ (1991): Hydrolysis of transforming growth factor-α by cell surface peptidases in vitro. Biochem J 280:57–60.

Cohen GM, Sun X-M, Fearnhead H, MacFarlane M, Brown DG, Snowden RT, Dinsdale D (1994): Formation of large molecular weight fragments of DNA is a key committed step of apoptosis in thymocytes. J Immunol 153:507–516.

Cohen GM, Sun X-M, Snowden RT, Ormerod MG, Dinsdale D (1993): Identification of a transitional preapoptotic population of thymocytes. J Immunol 151:566–574.

Darzynkiewicz Z, Bruno S, Del Bino G, Gorczyca W, MA, Lassota P, Traganos F (1992): Features of apoptotic cells measured by flow cytometry. Cytometry 13:795–808.

Dransfield I, Buckle AM, Savill JS, McDowall A, Haslett C, Hogg N (1994): Neutrophil apoptosis is associated with a reduction in CD16 (FcγrIII) expression. J Immunol 153: 1254–1263.

Duvall E, Wyllie H, Morris RG (1985): Macrophage recognition of cells undergoing programmed cell death (apoptosis). Immunology 56:351–358.

Ehlers MRW, Riordan JF (1991): Membrane proteins with soluble counterparts: role of proteolysis in the release of transmembrane proteins. Biochemistry 30:10065–1074.

Ellem KAO, Cullinan M, Baumann KC, Dunstan A (1988): UVR induction of TGF-alpha. A possible autocrine mechanism for the epidermal melanocytic response and for promotion of epidermal carcinogenesis. Carcinogenesis 9:797–801.

Fadok VA, Voelker DR, Campbell PA, Cohen JJ, Bratton DL, Henson PM (1992a): Exposure of phosphatidylserine on the surface of apoptotic lymphocytes triggers specific recognition and removal by macrophages. J Immunol 148:2207–2216.

Fadok VA, Savill JS, Haslett C, Bratton DL, Doherty DE, Campbell PA, Henson PM (1992b): Different populations of macrophages use either the vitronectin receptor or the phosphatidylserine receptor to recognize and remove apoptotic cells. J Immunol 149:4029–4035.

Harano T, Mizuno K (1994): Phorbol ester-induced activation of a membrane-bound candidate pro-transforming growth factor-α processing enzyme. J Biol Chem 269: 20305–20311.

Harmon BV, Corder AM, Collins RJ, Gobe GC, Allen J, Allan DJ, Kerr JFR (1990): Cell death induced in a murine mastocytoma by 42–47°C heating in vitro: Evidence that the form of death changes from apoptosis to necrosis above a critical heat load. Int J Radiat Biol 58:845–858.

Harrison D, Phillips JH, Lanier LL (1991): Involvement of a metaloprotease in spontaneous and phorbol ester-induced release of natural killer cell-associated FCγRIII. J Immunol 147:3459–3465.

Ignotz RA, Kelly B, Davis RJ, Massagué J (1986): Biologically active precursor for transforming growth factor type α, released by retrovirally transformed cells. Proc Natl Acad Sci 83:6307–6311.

Kenny AJ, O'Hare MJ, Gusterson BA (1989): Cell-surface peptidases as modulators of growth and differentiation. Lancet 12:785–787.

Kerr JFR, Wyllie AH, Currie AR (1972): Apoptosis: A basic biological phenomenon with wide-ranging implications in tissue kinetics. Br J Cancer 26:239–257.

Kerr JFR, Gobe GC, Winterford CM, Harmon BV (1995): Anatomical methods in cell death. Methods Cell Biol 64:1–27.

Kluck RM, Chapman DE, Egan M, McDougall CA, Harmon BV, Moss DJ, Kerr JFR, Halliday JW (1993): Spontaneous apoptosis in NS-1 myeloma cultures: Effects of cell density, conditioned medium and acid pH. Immunobiology 188:124–133.

Lennon SV, Martin SJ, Cotter TG (1991): Dose-dependent induction of apoptosis in human tumour cell lines by widely diverging stimuli. Cell Prolif 24:203–214.

Louvard D, Maroux S, Vannier CH, Desnuelle P (1975): Topological studies on the hydrolases to the intestinal brush border membrane. Biochim Biophys Acta 375:236–248.

Massagué J (1990): Transforming growth factor-α. J Biol Chem 265:21393–21396.

Massagué J, Pandiella A (1993): Membrane-anchored growth factors. Annu Rev Biochem 62:515–541.

Menrad A, Speicher D, Wacker J, Herlyn M (1993): Biochemical and functional characterization of aminopeptidase-N expressed by human melanoma cells. Cancer Res 53:1450–1455.

Mueller SG, Paterson AJ, Kudlow JE (1990): Transforming growth factor α in arterioles: Cell surface processing of its precursor by elastases. Mol Cell Biol 10:4596–4602.

Oberhammer F, Wilson JW, Dive C, Morris ID, Hickman JA, Wakeling AE, Walker PR, Sikorska M (1993): Apoptotic death in epithelial cells: Cleavage of DNA to 300 and/or 50 kb fragments prior to or in the absence of internucleosomal fragmentation. EMBO J 12:3679–3684.

Ormerod MG, Sun X-M, Snowden RT, Davies R, Fearnhead H, Cohen GM (1993): Increased membrane permeability of apoptotic thymocytes: A flow cytometric study. Cytometry 14:595–602.

Pandiella A, Bosenberg MW, Huang EJ, Besmer P, Massagué J (1992): Cleavage of membrane-anchored growth factors involves distinct protease activities regulated through common mechanisms. J Biol Chem 267:24028–20433.

Plakidou-Dymock S, Tanner MJ, McGivan JD (1993): A role for aminopeptidase N in Na^+-dependent amino acid transport in bovine renal brush-border membranes. Biochem J 290:59–65.

Rotello RJ, Fernandez PA, Yuan J (1994): Anti-apogens and anti-engulfens: Monoclonal antibodies reveal specific antigens on apoptotic and engulment cells during chicken embryonic development. Development 120:1421–1431.

Saiki I, Fujii H, Yoneda J, Abe F, Nakajima M, Tsuruo T, Azuma I (1993): Role of aminopeptidase-N (CD13) in tumor-cell Invasion and extracellular matrix degradation. Int J Cancer 54:137–143.

Savill J, Fadok V, Henson P, Haslett C (1993): Phagocyte recognition of cells undergoing apoptosis. Immunol Today 14:131–136.

Suda H, Aoyagi T, Takeuchi T, Umezawa H (1976): Inhibition of aminopeptidase-B and leucine aminopeptidase by bestatin and its stereoisomer. Arch Biochem Biophys 177: 196–200.

Sun X-M, Snowden RT, Skilleter DN, Dinsdale D, Ormerod MG, Cohen GM (1993): A flow-cytometric method for the separation and quantitation of normal and apoptotic thymocytes. Anal Biochem 204:351–356.

Tomei LD, Shapiro JP, Cope FO (1993): Apoptosis in C3H/10T½ mouse embryonic cells: Evidence of internucleosomal DNA modification in the absence of double-strand cleavage. Proc Natl Acad Sci USA 90:853–857.

Walker NI, Harmon BV, Gobe GC, Kerr JFR (1988): Patterns of cell death. Methods Ach Exp Pathol 13:18–54.

Walker PR, Kokileva L, LeBlanc J, Sikorska M (1994): Detection of the initial stages of DNA fragmentation in apoptosis. Biotechniques 15:1032–1040.

Wyllie AH (1993): Apoptosis (The 1992 Frank Rose Memorial Lecture). Br J Cancer 67:205–208.